Strål
säkerhets
myndigheten
Swedish Radiation Safety Authority

Authors: Jeoung Seok Yoon[1], Ove Stephansson[1] and Ki-Bok Min[2]
[1] Stephansson Rock Consultant, Berlin, Germany
[2] Seoul National University, Seoul, South Korea

Technical Note 74; page 163-190

2014:59

Relation between earthquake magnitude, fracture length and fracture shear displacement in the KBS-3 repository at Forsmark

Main Review Phase

Date: December 2014
Report number: 2014:59 **ISSN:** 2000-0456
Available at www.stralsakerhetsmyndigheten.se

Models in Section 6.2

Earthquake induced, ZFMWNW0809A, glacial induced stress at the time of forebulge, DFN03h

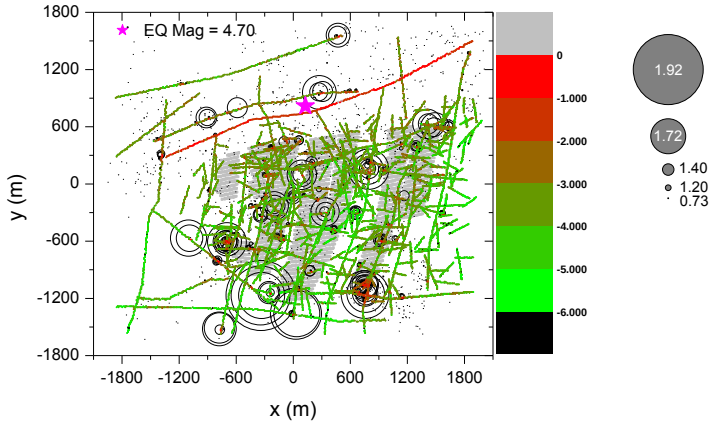

Figure A3-47. Spatial distribution of the induced seismic events and shear displacement of the joint planes that constitute the TFs and DZs, due to seismic event at zone ZFMWNW0809A with realization DFN03h.

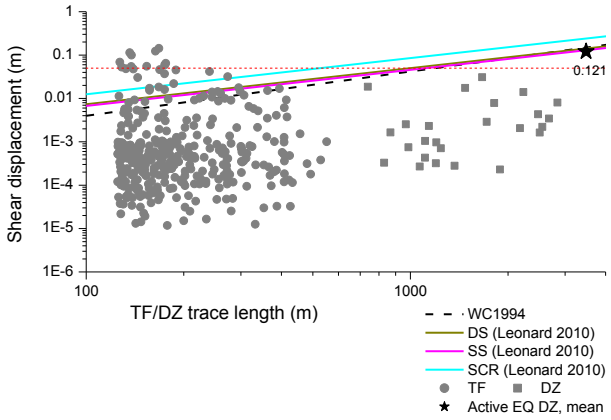

Figure A3-48. Shear displacement of the TFs and DZs with respect to length, due to seismic event at zone ZFMWNW0809A with realization DFN03h and comparison with empirical regressions.

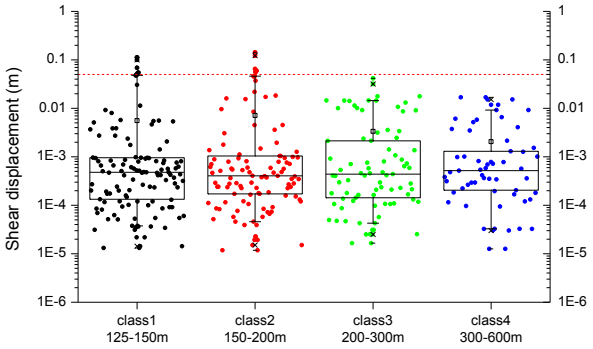

Figure A3-49. Box-and-whisker diagram of the TF shear displacement in four trace length classes, due to seismic event at zone ZFMWNW0809A with realization DFN03h.

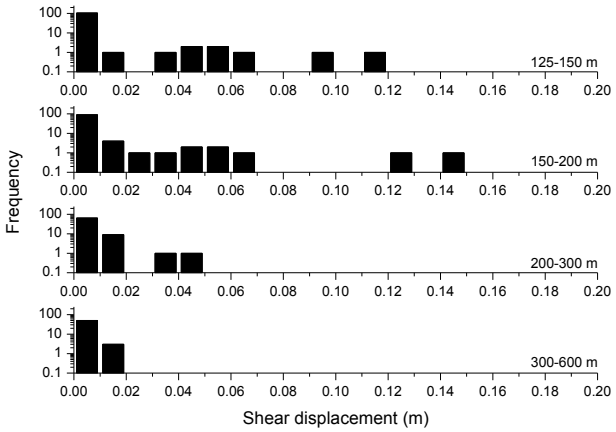

Figure A3-50. Histogram of shear displacement of the TFs in four different trace length classes, due to seismic event at zone ZFMWNW0809A with realization DFN03h.

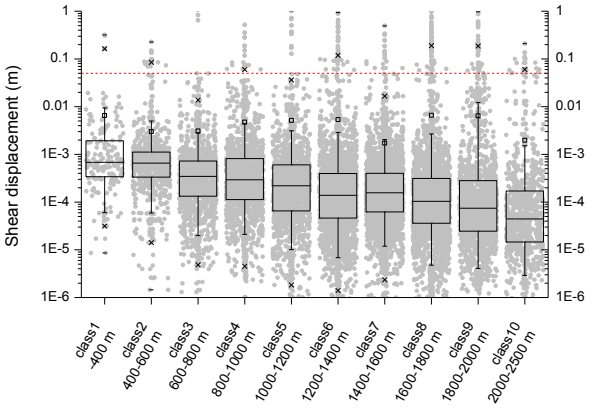

Figure A3-51. Box-and-whisker diagram of the shear displacement of smooth joints of TFs in nine classes of distance from the hypocentre of simulated earthquake.

Earthquake induced, ZFMWNW0809A, glacial induced stress at the time of forebulge, DFN06h

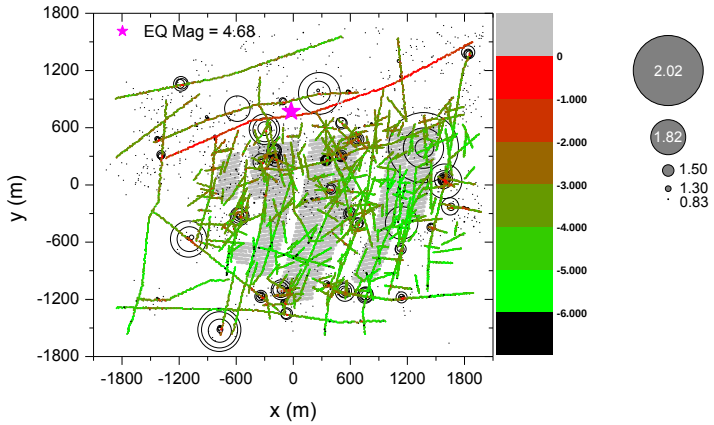

Figure A3-52. Spatial distribution of the induced seismic events and shear displacement of the joint planes that constitute the TFs and DZs, due to seismic event at zone ZFMWNW0809A with realization DFN06h.

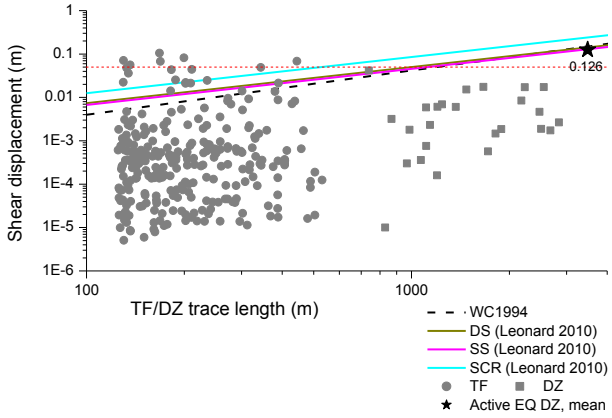

Figure A3-53. Shear displacement of the TFs and DZs with respect to length, due to seismic event at zone ZFMWNW0809A with realization DFN06h and comparison with empirical regressions.

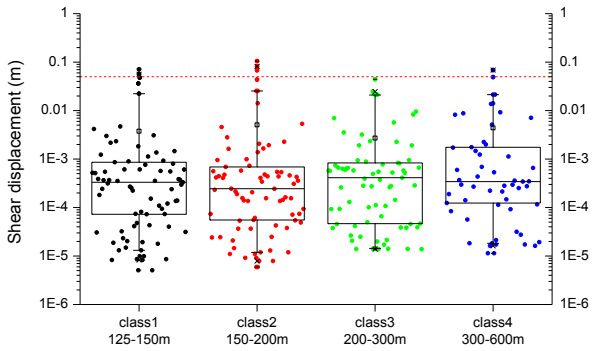

Figure A3-54. Box-and-whisker diagram of the TF shear displacement in four trace length classes, due to seismic event at zone ZFMWNW0809A with realization DFN06h.

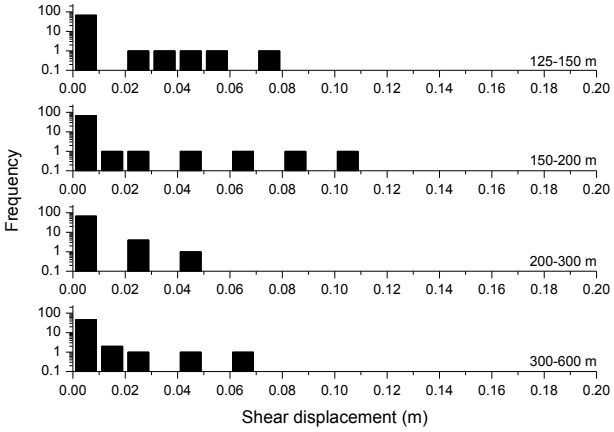

Figure A3-55. Histogram of shear displacement of the TFs in four different trace length classes, due to seismic event at zone ZFMWNW0809A with realization DFN06h.

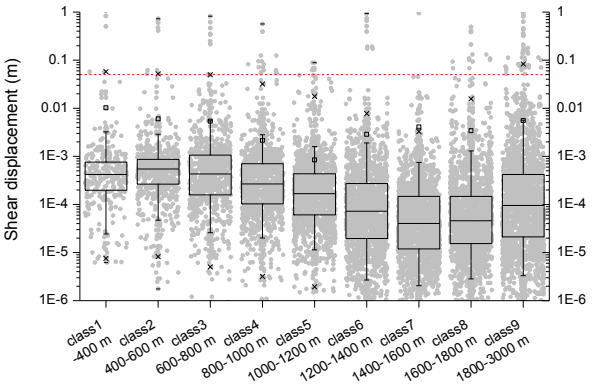

Figure A3-56. Box-and-whisker diagram of the shear displacement of smooth joints of TFs in nine classes of distance from the hypocentre of simulated earthquake.

Earthquake induced, ZFMWNW0001, glacial induced stress at the time of forebulge, DFN03h, powered shear force

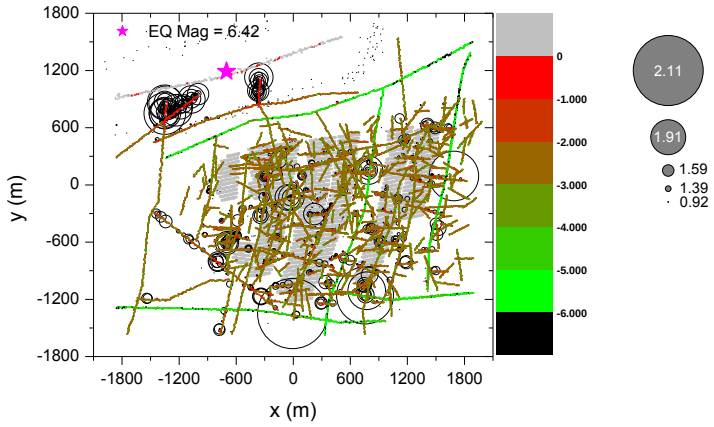

Figure A3-57. Spatial distribution of the induced seismic events and shear displacement of the joint planes that constitute the TFs and DZs, due to seismic event at zone ZFMWNW0001 with realization DFN03h.

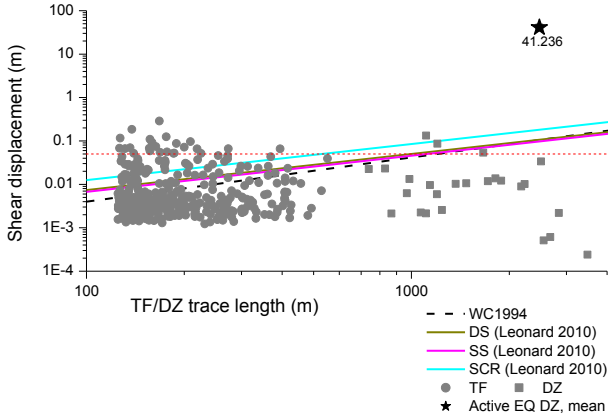

Figure A3-58. Shear displacement of the TFs and DZs with respect to length, due to seismic event at zone ZFMWNW0001 with realization DFN03h and comparison with empirical regressions.

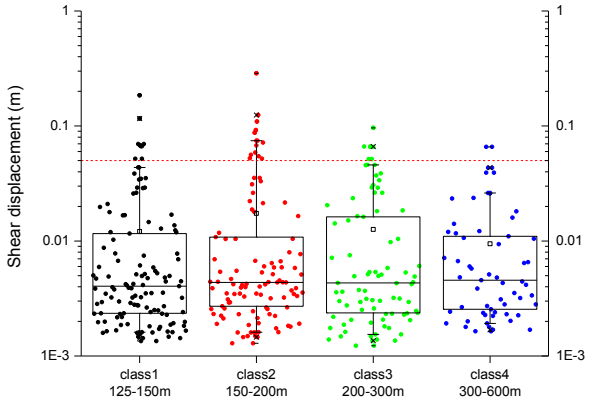

Figure A3-59. Box-and-whisker diagram of the TF shear displacement in four trace length classes, due to seismic event at zone ZFMWNW0001 with realization DFN03h.

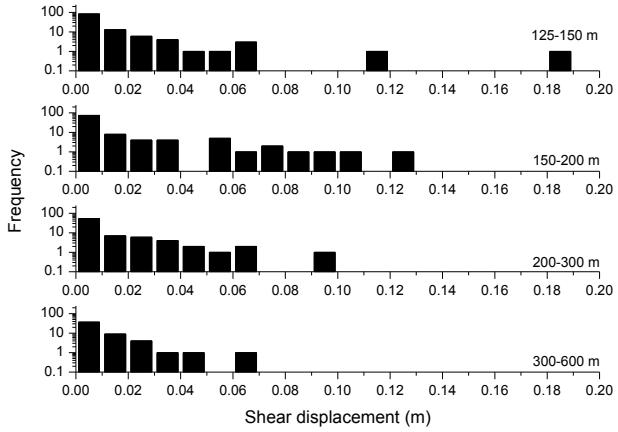

Figure A3-60. Histogram of shear displacement of the TFs in four different trace length classes, due to seismic event at zone ZFMWNW0001 with realization DFN03h.

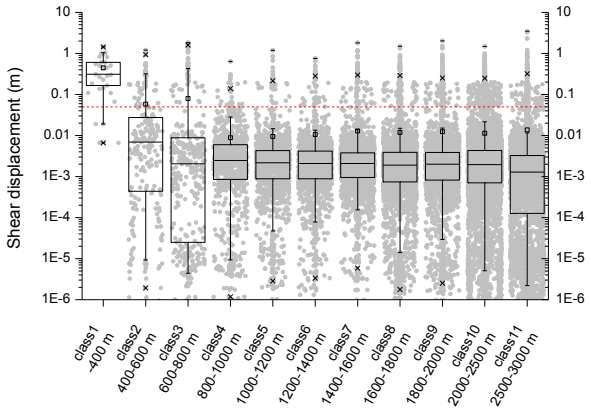

Figure A3-61. Box-and-whisker diagram of the shear displacement of smooth joints of TFs in six classes of distance from the hypocentre of simulated earthquake.

Earthquake induced, ZFMWNW0001, glacial induced stress at the time of forebulge, DFN06h, powered shear force

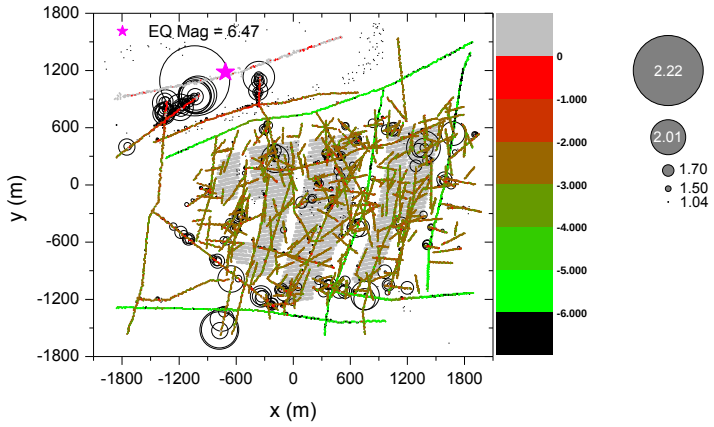

Figure A3-62. Spatial distribution of the induced seismic events and shear displacement of the joint planes that constitute the TFs and DZs, due to seismic event at zone ZFMWNW0001 with realization DFN06h.

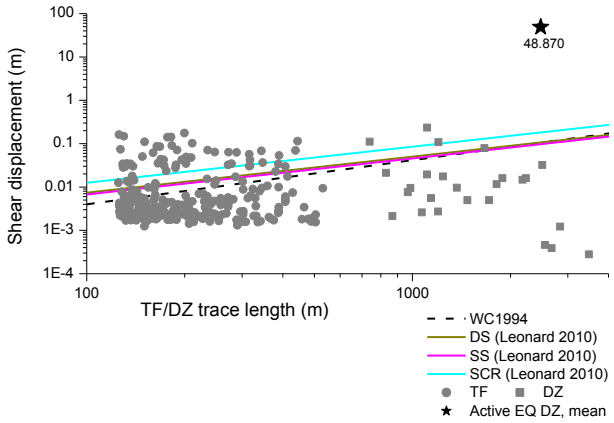

Figure A3-63. Shear displacement of the TFs and DZs with respect to length, due to seismic event at zone ZFMWNW0001 with realization DFN06h and comparison with empirical regressions.

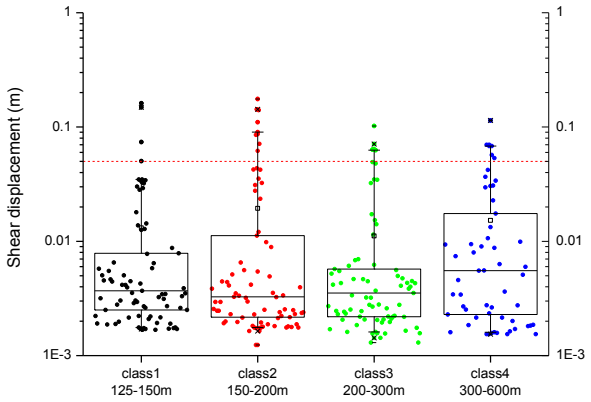

Figure A3-64. Box-and-whisker diagram of the TF shear displacement in four trace length classes, due to seismic event at zone ZFMWNW0001 with realization DFN06h.

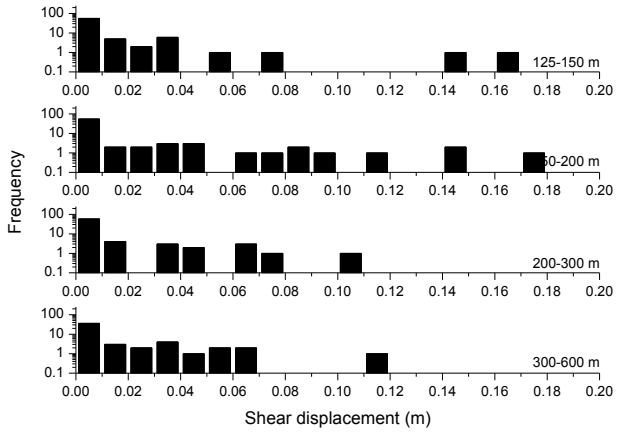

Figure A3-65. Histogram of shear displacement of the TFs in four different trace length classes, due to seismic event at zone ZFMWNW0001 with realization DFN06h.

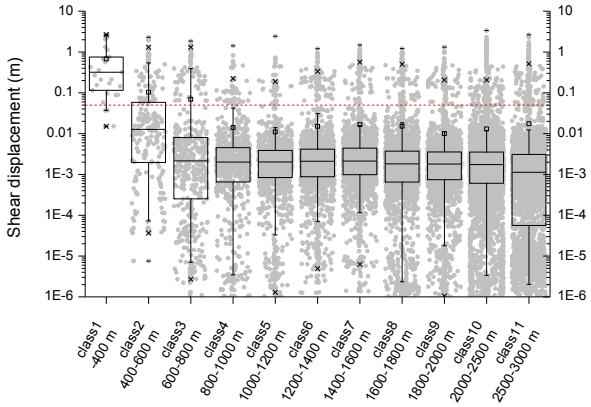

Figure A3-66. Box-and-whisker diagram of the shear displacement of smooth joints of TFs in six classes of distance from the hypocentre of simulated earthquake.

Earthquake induced, ZFMWNW2225, glacial induced stress at the time of forebulge, DFN03h

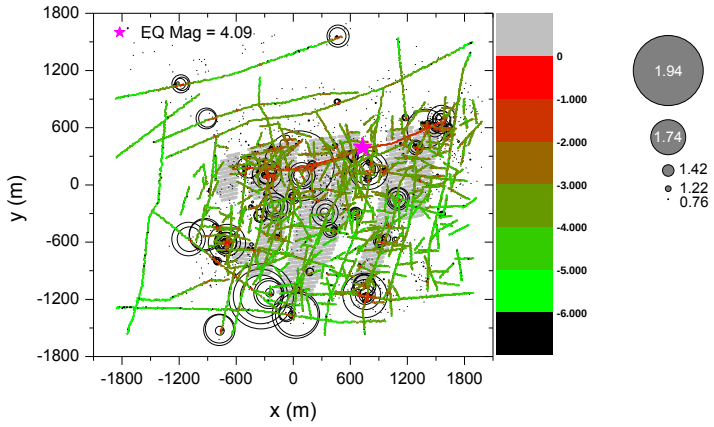

Figure A3-67. Spatial distribution of the induced seismic events and shear displacement of the joint planes that constitute the TFs and DZs, due to seismic event at zone ZFMWNW2225 with realization DFN03h.

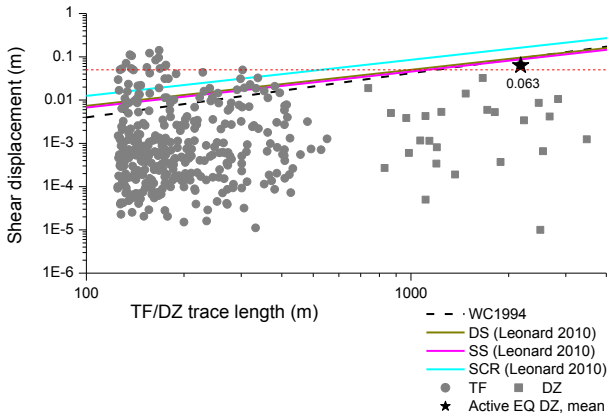

Figure A3-68. Shear displacement of the TFs and DZs with respect to length, due to seismic event at zone ZFMWNW2225 with realization DFN03h and comparison with empirical regressions.

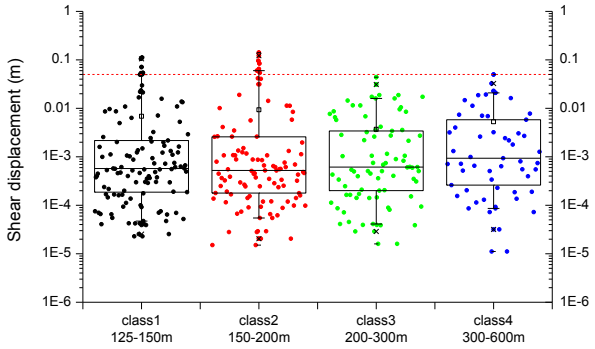

Figure A3-69. Box-and-whisker diagram of the TF shear displacement in four trace length classes, due to seismic event at zone ZFMWNW2225 with realization DFN03h.

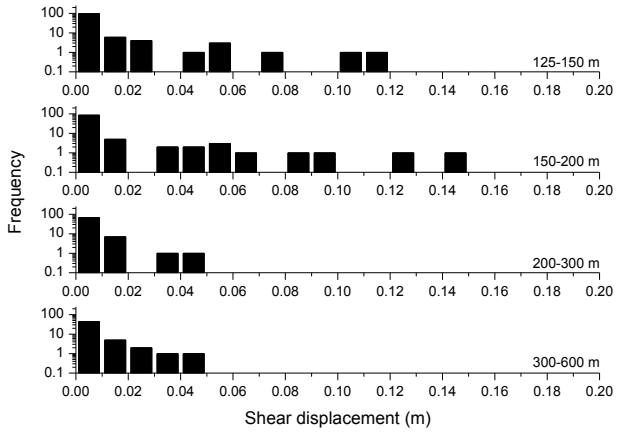

Figure A3-70. Histogram of shear displacement of the TFs in four different trace length classes, due to seismic event at zone ZFMWNW2225 with realization DFN03h.

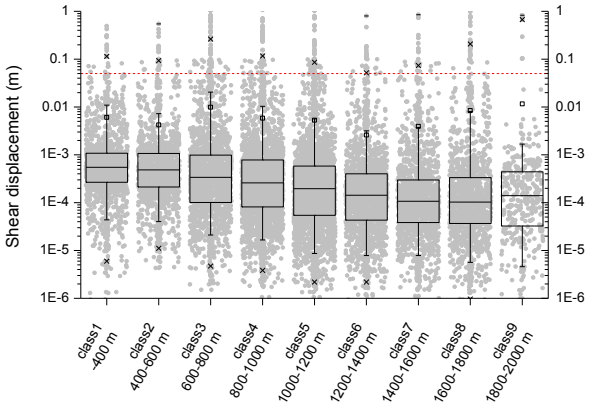

Figure A3-71. Box-and-whisker diagram of the shear displacement of smooth joints of TFs in nine classes of distance from the hypocentre of simulated earthquake.

Earthquake induced, ZFMWNW2225, glacial induced stress at the time of forebulge, DFN06h

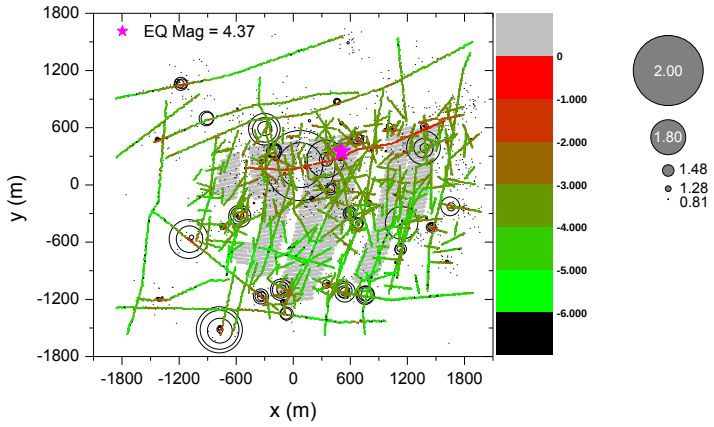

Figure A3-72. Spatial distribution of the induced seismic events and shear displacement of the joint planes that constitute the TFs and DZs, due to seismic event at zone ZFMWNW2225 with realization DFN06h.

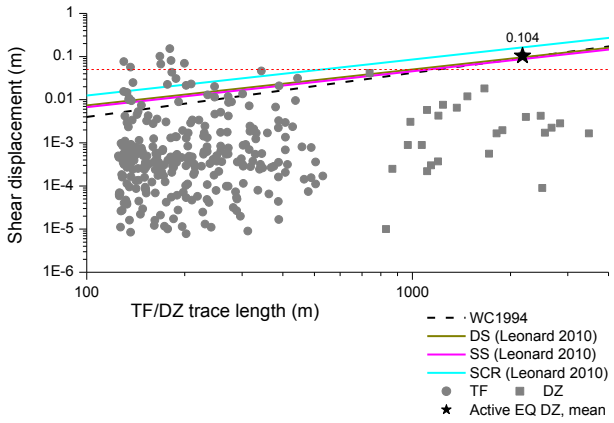

Figure A3-73. Shear displacement of the TFs and DZs with respect to length, due to seismic event at zone ZFMWNW2225 with realization DFN06h and comparison with empirical regressions.

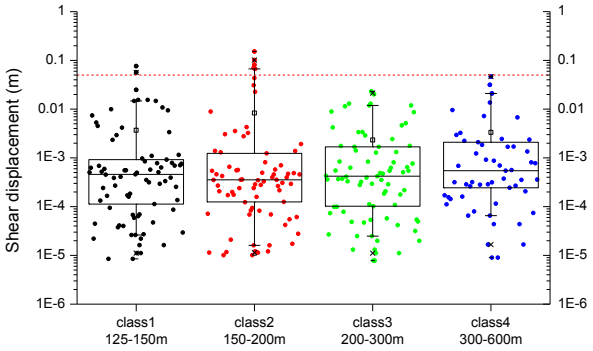

Figure A3-74. Box-and-whisker diagram of the TF shear displacement in four trace length classes, due to seismic event at zone ZFMWNW2225 with realization DFN06h.

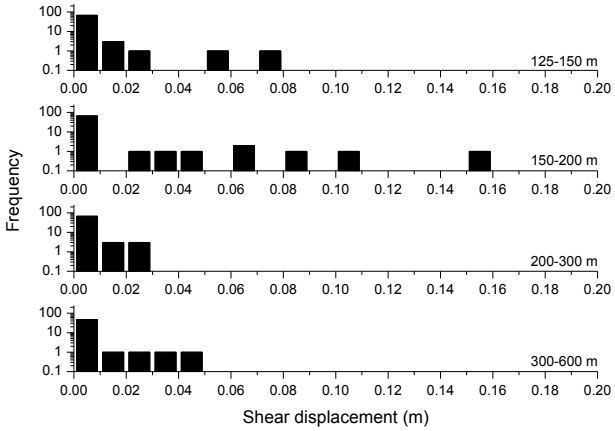

Figure A3-75. Histogram of shear displacement of the TFs in four different trace length classes, due to seismic event at zone ZFMWNW2225 with realization DFN06h.

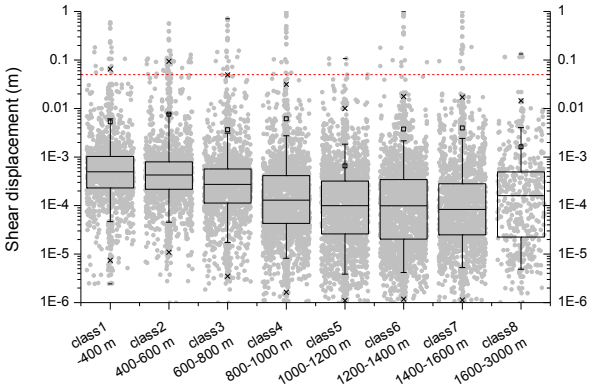

Figure A3-76. Box-and-whisker diagram of the shear displacement of smooth joints of TFs in nine classes of distance from the hypocentre of simulated earthquake.

Earthquake induced, ZFMNW1200, glacial induced stress at the time of forebulge, DFN03h

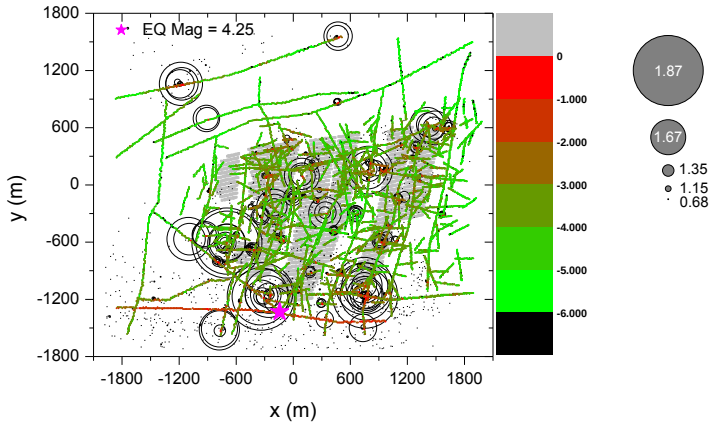

Figure A3-77. Spatial distribution of the induced seismic events and shear displacement of the joint planes that constitute the TFs and DZs, due to seismic event at zone ZFMNW1200 with realization DFN03h.

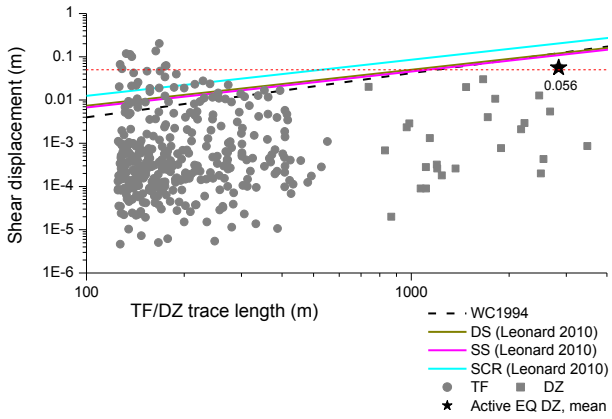

Figure A3-78. Shear displacement of the TFs and DZs with respect to length, due to seismic event at zone ZFMNW1200 with realization DFN03h and comparison with empirical regressions.

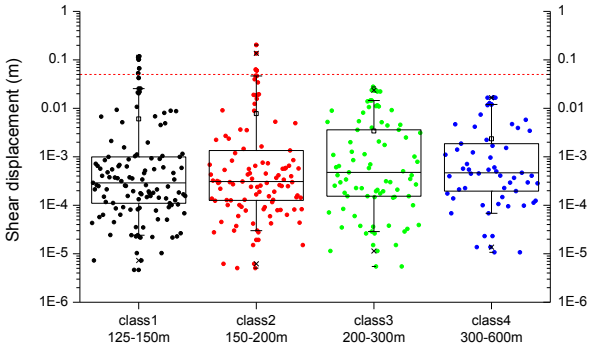

Figure A3-79. Box-and-whisker diagram of the TF shear displacement in four trace length classes, due to seismic event at zone ZFMNW1200 with realization DFN03h.

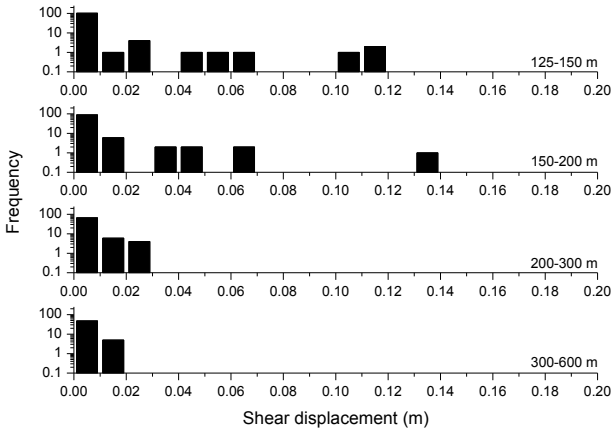

Figure A3-80. Histogram of shear displacement of the TFs in four different trace length classes, due to seismic event at zone ZFMNW1200 with realization DFN03h.

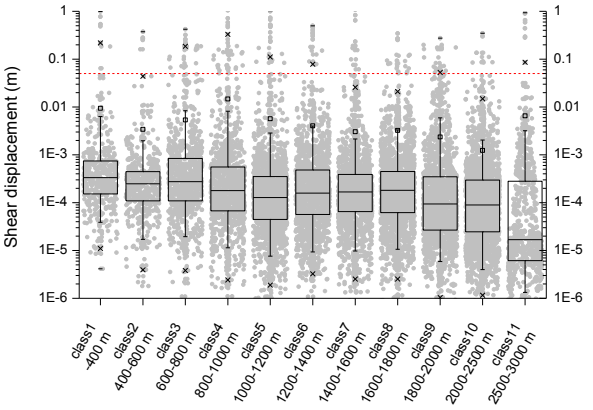

Figure A3-81. Box-and-whisker diagram of the shear displacement of smooth joints of TFs in seven classes of distance from the hypocentre of simulated earthquake.

Earthquake induced, ZFMNW1200, glacial induced stress at the time of forebulge, DFN06h

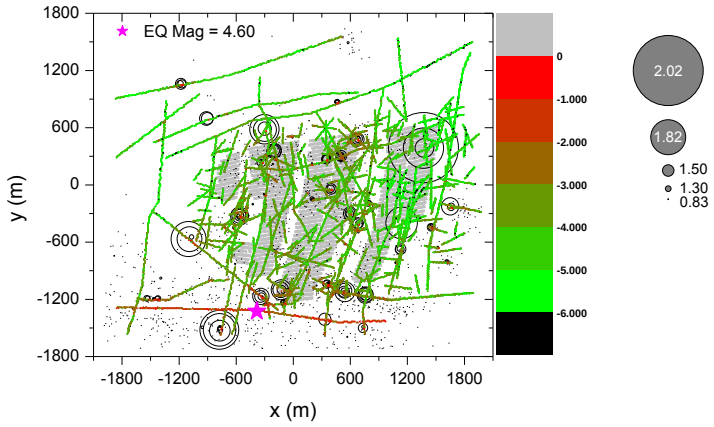

Figure A3-82. Spatial distribution of the induced seismic events and shear displacement of the joint planes that constitute the TFs and DZs, due to seismic event at zone ZFMNW1200 with realization DFN06h.

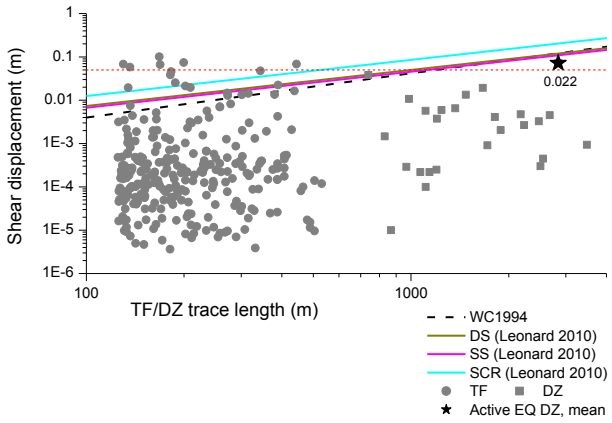

Figure A3Figure A3-83. Shear displacement of the TFs and DZs with respect to length, due to seismic event at zone ZFMNW1200 with realization DFN06h and comparison with empirical regressions.

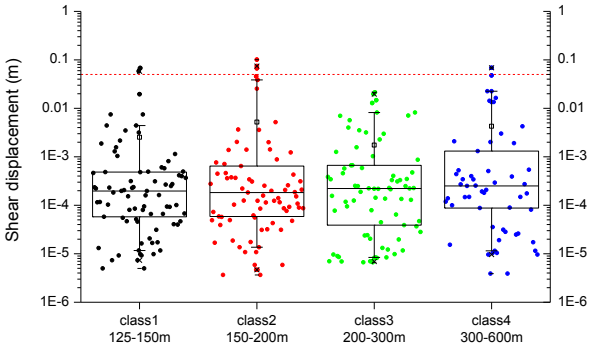

Figure A3-84. Box-and-whisker diagram of the TF shear displacement in four trace length classes, due to seismic event at zone ZFMNW1200 with realization DFN06h.

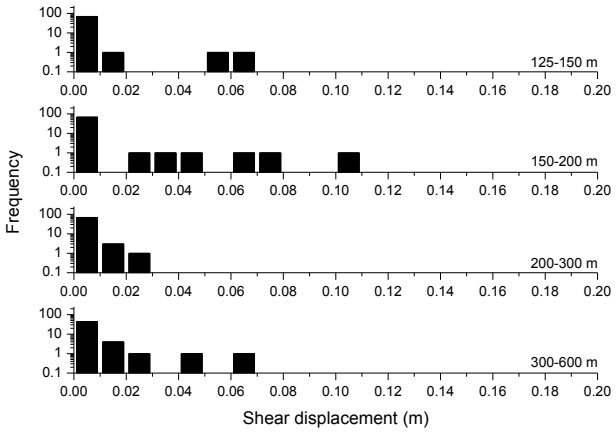

Figure A-85. Histogram of shear displacement of the TFs in four different trace length classes, due to seismic event at zone ZFMNW1200 with realization DFN06h.

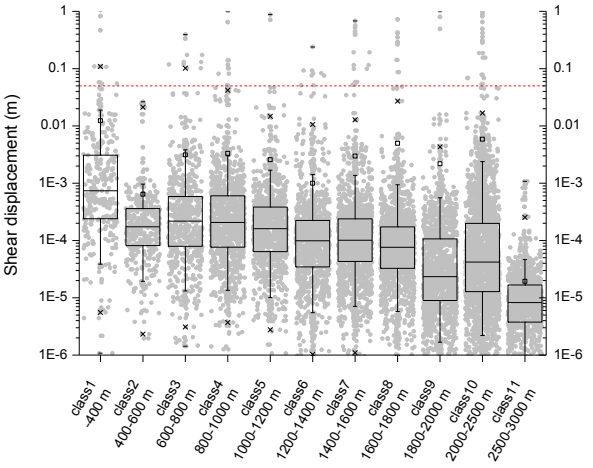

Figure A3-86. Box-and-whisker diagram of the shear displacement of smooth joints of TFs in six classes of distance from the hypocentre of simulated earthquake.

Models in Section 6.3

Earthquake induced, ZFMWNW0809A, glacial induced stress at the time of maximum thickness of ice cover, DFN03h

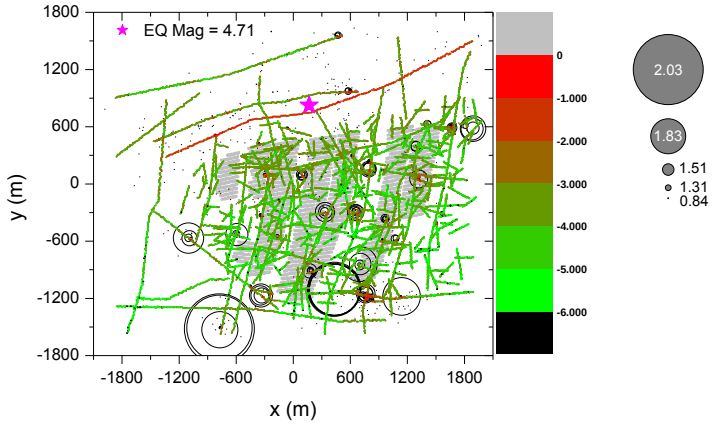

Figure A3-87. Spatial distribution of the induced seismic events and shear displacement of the joint planes that constitute the TFs and DZs, due to seismic event at zone ZFMWNW0809A with realization DFN03h.

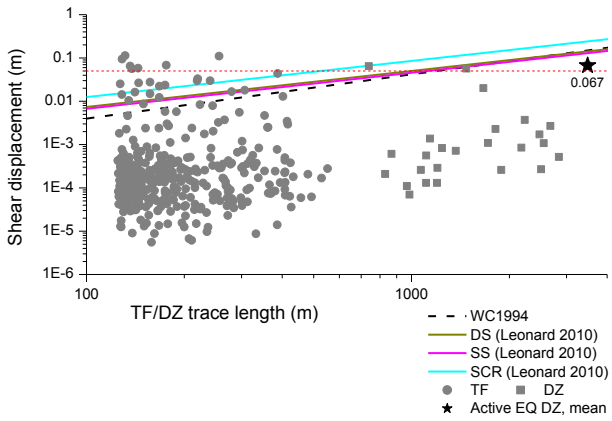

Figure A3-88. Shear displacement of the TFs and DZs with respect to length, due to seismic event at zone ZFMWNW0809A with realization DFN03h and comparison with empirical regressions.

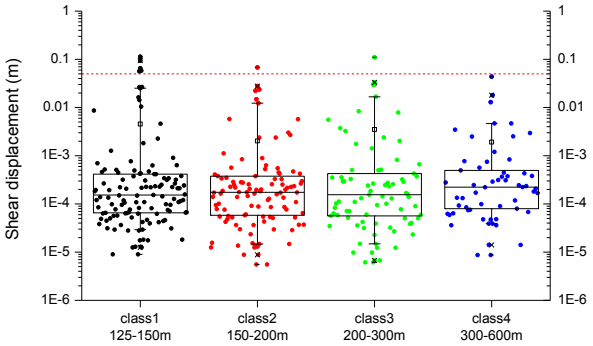

Figure A3-89. Box-and-whisker diagram of the TF shear displacement in four trace length classes, due to seismic event at zone ZFMWNW0809A with realization DFN03h.

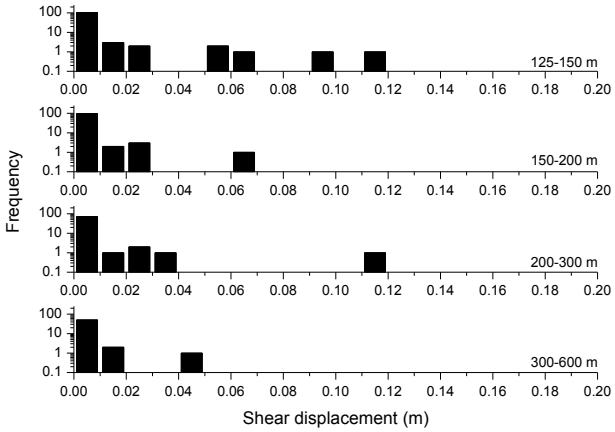

Figure A3-90. Histogram of shear displacement of the TFs in four different trace length classes, due to seismic event at zone ZFMWNW0809A with realization DFN03h.

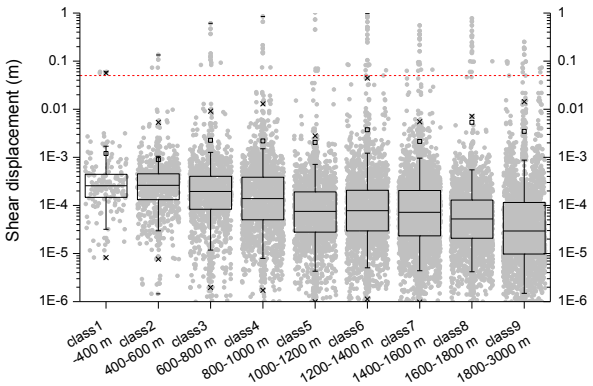

Figure A3-91. Box-and-whisker diagram of the shear displacement of smooth joints of TFs in nine classes of distance from the hypocentre of simulated earthquake.

Earthquake induced, ZFMWNW0809A, glacial induced stress at the time of maximum thickness of ice cover, DFN06h

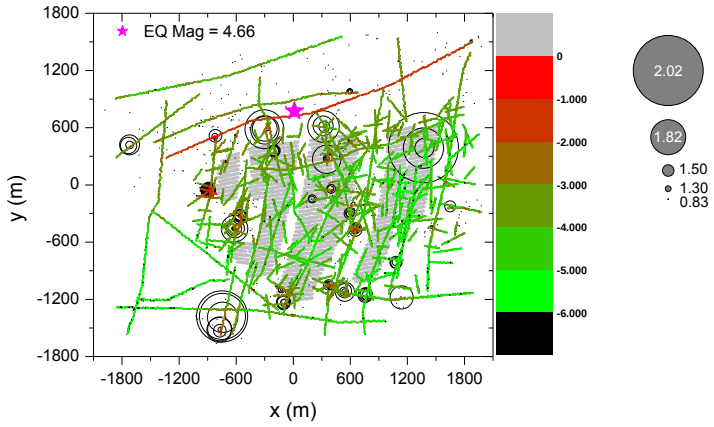

Figure A3-92. Spatial distribution of the induced seismic events and shear displacement of the joint planes that constitute the TFs and DZs, due to seismic event at zone ZFMWNW0809A with realization DFN06h.

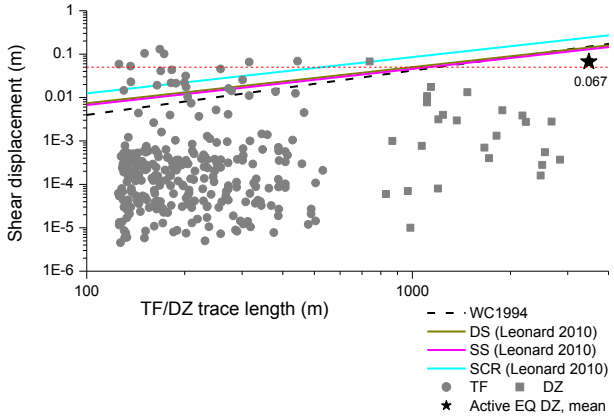

Figure A3-93. Shear displacement of the TFs and DZs with respect to length, due to seismic event at zone ZFMWNW0809A with realization DFN06h and comparison with empirical regressions.

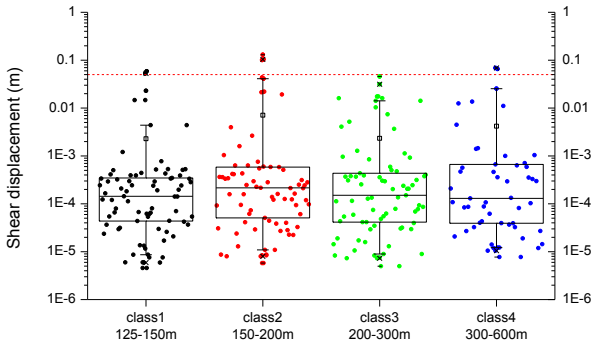

Figure A3-94. Box-and-whisker diagram of the TF shear displacement in four trace length classes, due to seismic event at zone ZFMWNW0809A with realization DFN06h.

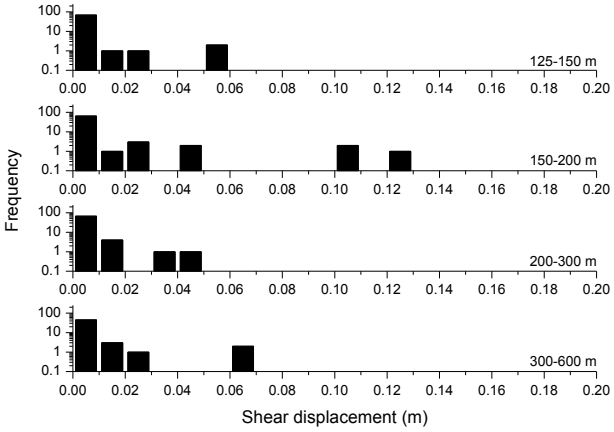

Figure A3-95. Histogram of shear displacement of the TFs in four different trace length classes, due to seismic event at zone ZFMWNW0809A with realization DFN06h.

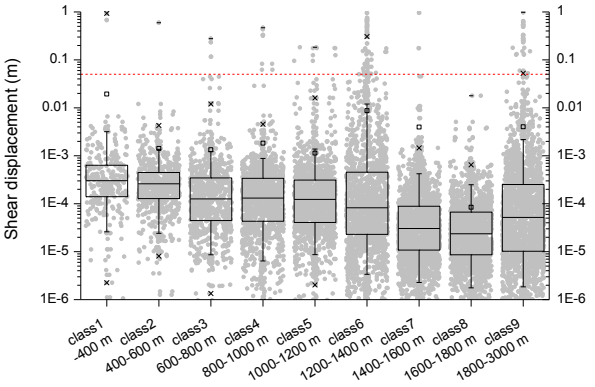

Figure A3-96. Box-and-whisker diagram of the shear displacement of smooth joints of TFs in nine classes of distance from the hypocentre of simulated earthquake.

Earthquake induced, ZFMWNW2225, glacial induced stress at the time of maximum thickness of ice cover, DFN03h

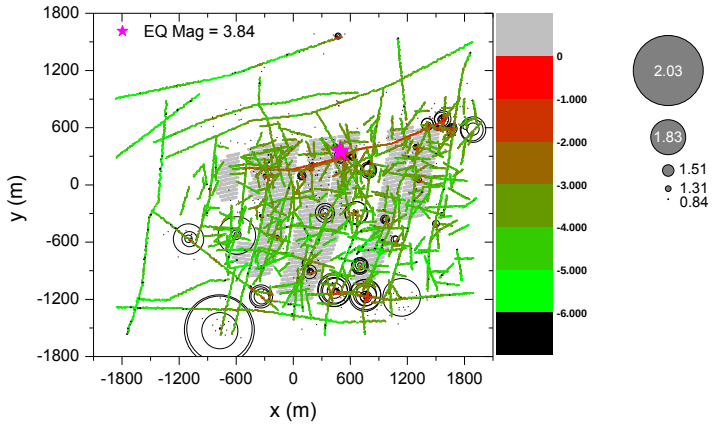

Figure A3-97. Spatial distribution of the induced seismic events and shear displacement of the joint planes that constitute the TFs and DZs, due to seismic event at zone ZFMWNW2225 with realization DFN03h.

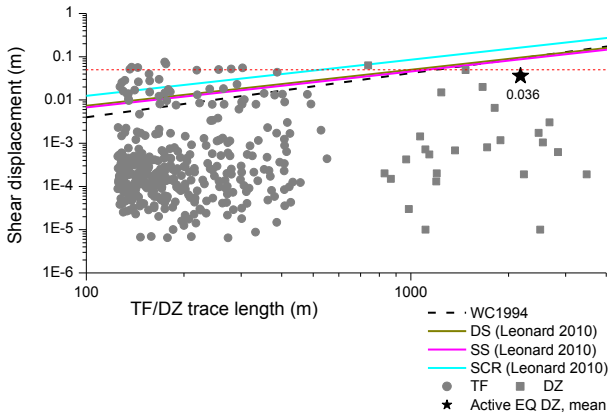

Figure A3-98. Shear displacement of the TFs and DZs with respect to length, due to seismic event at zone ZFMWNW2225 with realization DFN03h and comparison with empirical regressions.

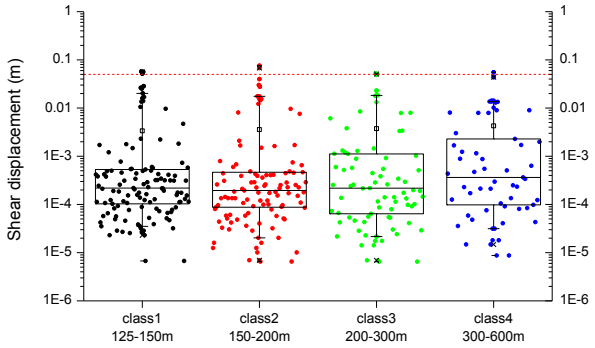

Figure A3-99. Box-and-whisker diagram of the TF shear displacement in four trace length classes, due to seismic event at zone ZFMWNW2225 with realization DFN03h.

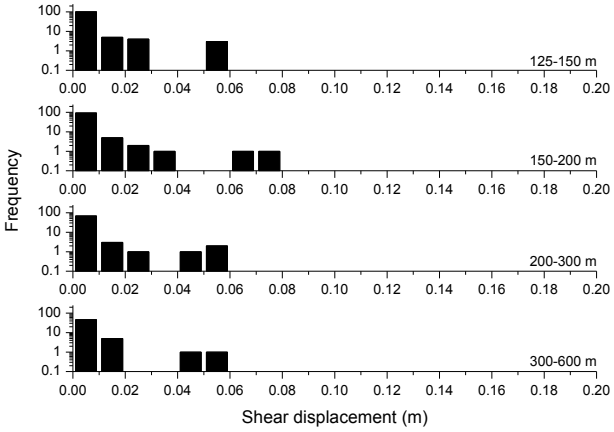

Figure A3-100. Histogram of shear displacement of the TFs in four different trace length classes, due to seismic event at zone ZFMWNW2225 with realization DFN03h.

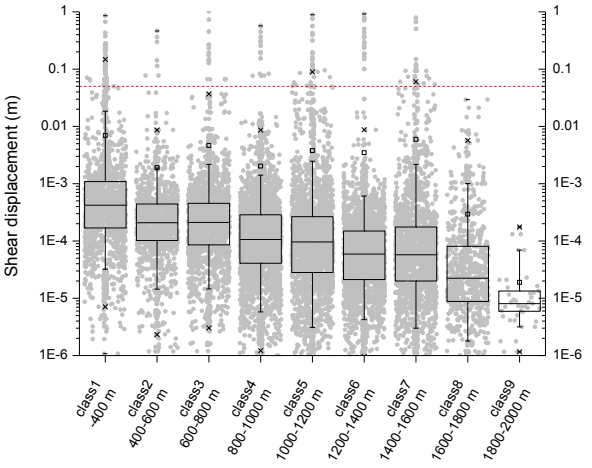

Figure A3-101. Box-and-whisker diagram of the shear displacement of smooth joints of TFs in nine classes of distance from the hypocentre of simulated earthquake.

Earthquake induced, ZFMWNW2225, glacial induced stress at the time of maximum thickness of ice cover, DFN06h

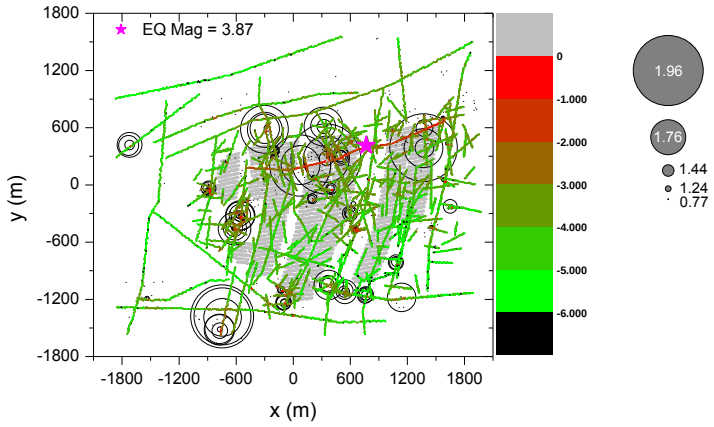

Figure A3-102. Spatial distribution of the induced seismic events and shear displacement of the joint planes that constitute the TFs and DZs, due to seismic event at zone ZFMWNW2225 with realization DFN06h.

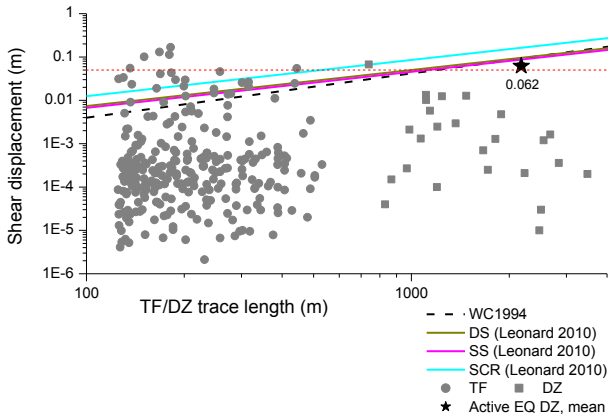

Figure A3-103. Shear displacement of the TFs and DZs with respect to length, due to seismic event at zone ZFMWNW2225 with realization DFN06h and comparison with empirical regressions.

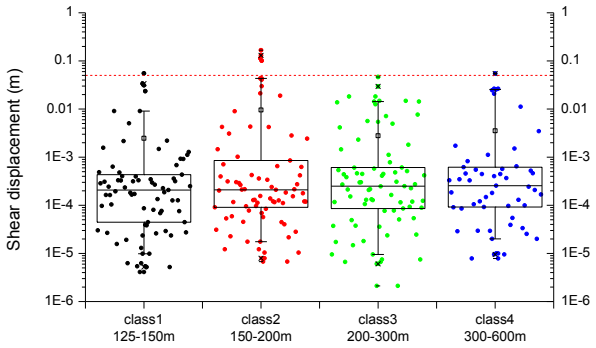

Figure A3-104. Box-and-whisker diagram of the TF shear displacement in four trace length classes, due to seismic event at zone ZFMWNW2225 with realization DFN06h.

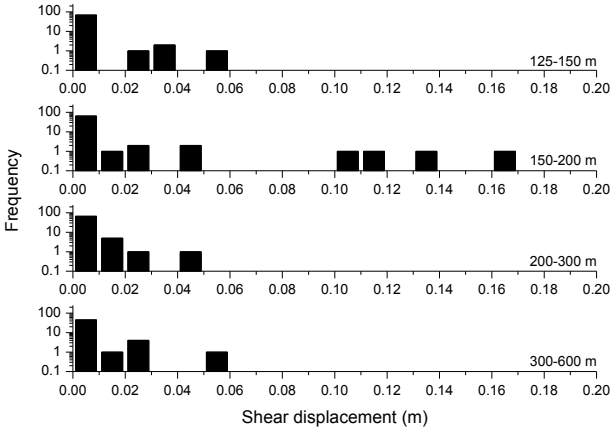

Figure A3-105. Histogram of shear displacement of the TFs in four different trace length classes, due to seismic event at zone ZFMWNW2225 with realization DFN06h.

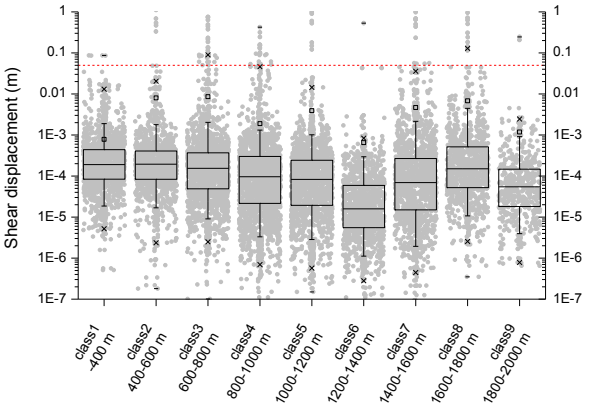

Figure A3-106. Box-and-whisker diagram of the shear displacement of smooth joints of TFs in eight classes of distance from the hypocentre of simulated earthquake.

Earthquake induced, ZFMNW1200, glacial induced stress at the time of maximum thickness of ice cover, DFN03h

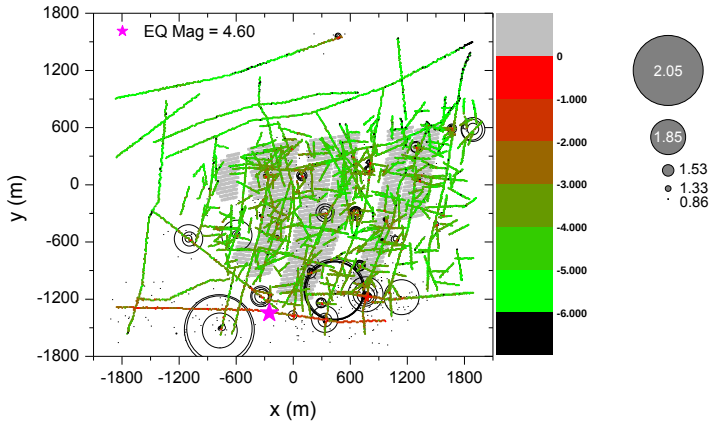

Figure A3-107. Spatial distribution of the induced seismic events and shear displacement of the joint planes that constitute the TFs and DZs, due to seismic event at zone ZFMNW1200 with realization DFN03h.

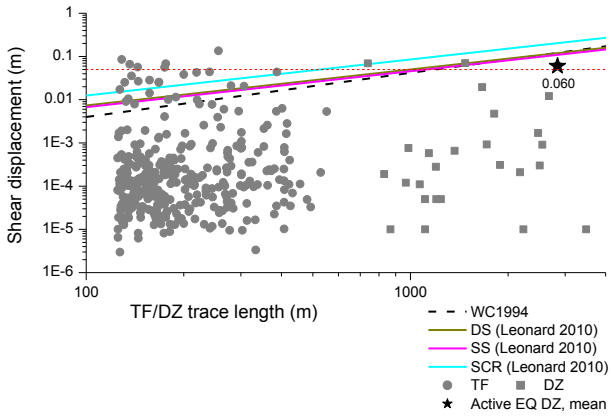

Figure A3-108. Shear displacement of the TFs and DZs with respect to length, due to seismic event at zone ZFMWW1200 with realization DFN03h and comparison with empirical regressions.

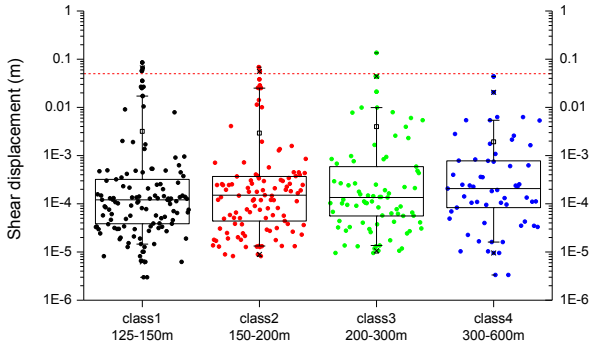

Figure A3-109. Box-and-whisker diagram of the TF shear displacement in four trace length classes, due to seismic event at zone ZFMNW1200 with realization DFN03h.

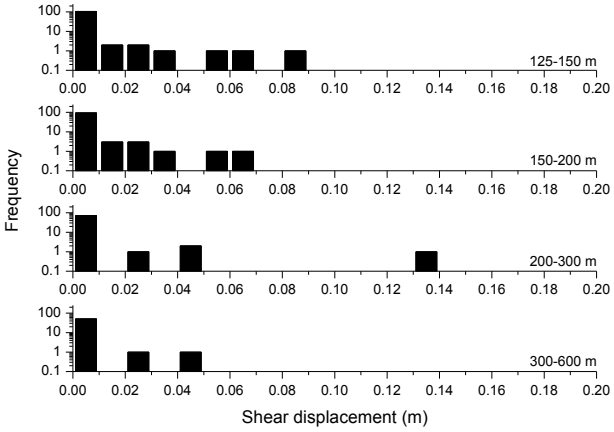

Figure A3-110. Histogram of shear displacement of the TFs in four different trace length classes, due to seismic event at zone ZFMNW1200 with realization DFN03h.

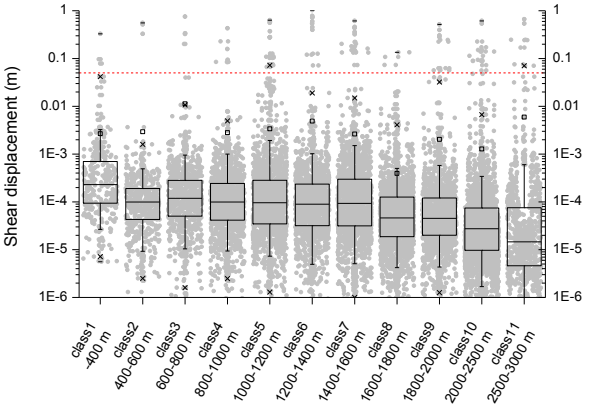

Figure A3-111. Box-and-whisker diagram of the shear displacement of smooth joints of TFs in six classes of distance from the hypocentre of simulated earthquake.

Earthquake induced, ZFMNW1200, glacial induced stress at the time of maximum thickness of ice cover, DFN06h

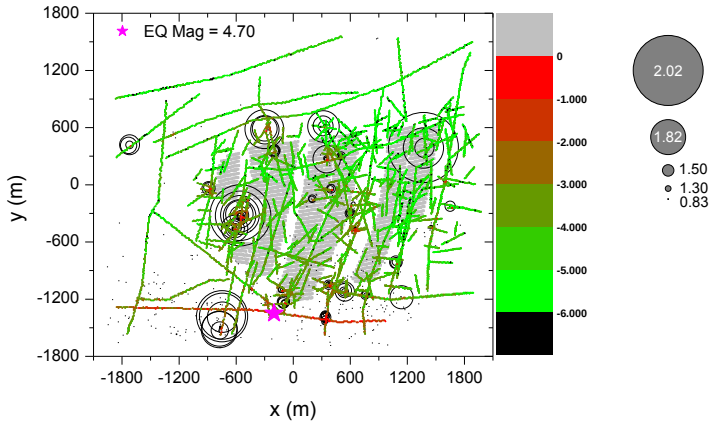

Figure A3-112. Spatial distribution of the induced seismic events and shear displacement of the joint planes that constitute the TFs and DZs, due to seismic event at zone ZFMNW1200 with realization DFN06h.

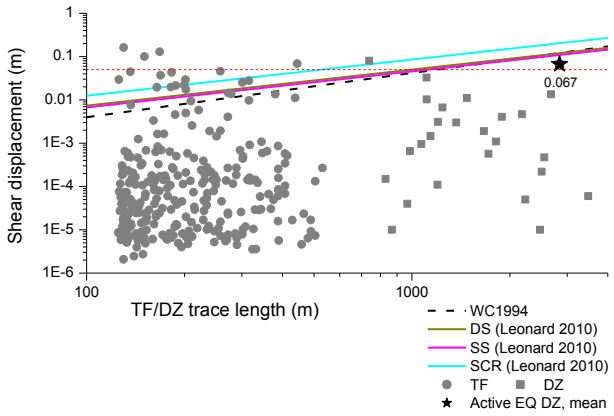

Figure A3-113. Shear displacement of the TFs and DZs with respect to length, due to seismic event at zone ZFMWW1200 with realization DFN06h and comparison with empirical regressions.

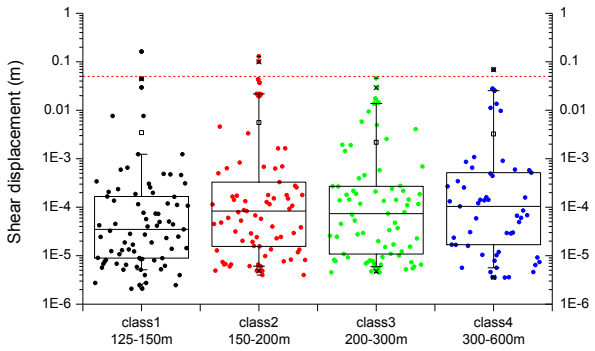

Figure A3-114. Box-and-whisker diagram of the TF shear displacement in four trace length classes, due to seismic event at zone ZFMNW1200 with realization DFN06h.

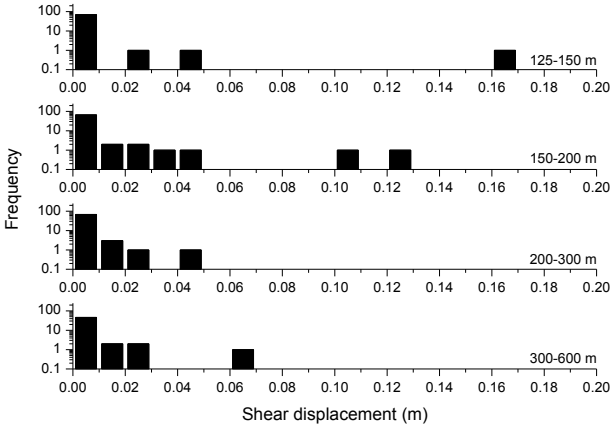

Figure A3-115. Histogram of shear displacement of the TFs in four different trace length classes, due to seismic event at zone ZFMNW1200 with realization DFN06h.

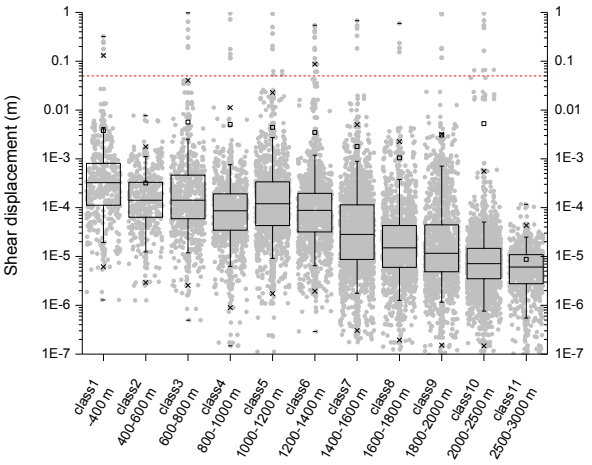

Figure A3-116. Box-and-whisker diagram of the shear displacement of smooth joints of TFs in five classes of distance from the hypocentre of simulated earthquake.